

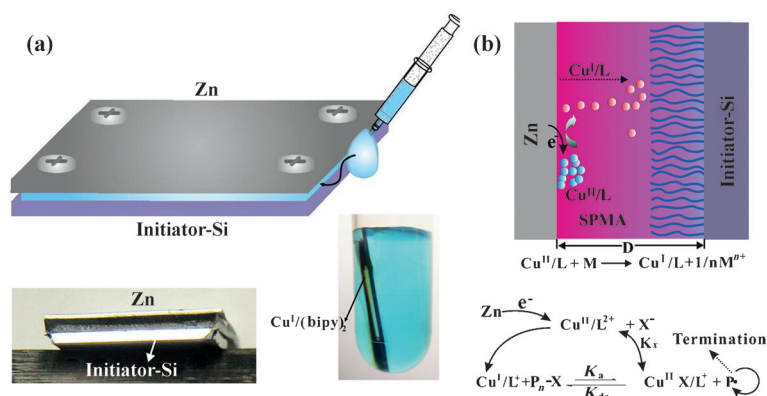
Controlled Polymer-Brush Growth from Microliter Volumes using Sacrificial-Anode Atom-Transfer Radical Polymerization**

Junfeng Yan, Bin Li, Bo Yu, Wilhelm T. S. Huck,* Weimin Liu,* and Feng Zhou*

Polymer brushes (i.e. polymer chains covalently tethered to the substrate at one end) have emerged as one of most useful and versatile routes to chemically functionalize substrates.^[1] Polymer brushes have been widely investigated to create surface coatings with tunable wettability and anti-biofouling,^[2] for protein immobilization,^[3] applications including filtration^[4] and actuation,^[5] and many other studies into the nanoscale properties of (patterned) polymer brushes.^[6] Typically, brushes form planar films, but locally changing the initiator grafting density using e-beam or dip-pen nanodisplacement lithography, leads to polymer films with gradients in thickness after polymerization.^[8] In addition to the formation of gradients, another major experimental challenge in the growth of polymer brushes is the extremely poor efficiency, in terms of monomer usage. Typically, milliliters of monomer solution are used to grow brush films in the range of (hundreds of) nanometers. This, combined with the requirement to grow brushes under controlled conditions, limits the use of precious monomers, as well as potential industrial applications.

Among different surface-polymerization strategies, surface-initiated atom-transfer radical polymerization (SI-ATRP) is one of the most versatile and widely used routes to prepare well-defined polymer brushes.^[7–9] Conventional SI-ATRP uses a Cu^I/ligand complex as the catalyst and must be carried out in an inert atmosphere to retain the activity of the catalyst.^[8,9] Recently, activators generated by electron-transfer ATRP (AGET-ATRP), electrochemically induced ATRP (eATRP), and light-induced ATRP were developed^[10–12] to enable ATRP by forming the Cu^I/ligand catalyst in situ. We have developed SI-

eATRP that allows polymer-brush grafting in an ambient atmosphere.^[13] However, this method requires an electrochemical setup and a large volume of solution. Herein, we report a novel approach to grow polymer brushes using small volumes (μL) of solution. As this method is reminiscent of the use of Zn as a sacrificial anode in corrosion engineering, we call our approach sacrificial-anode ATRP (sa-ATRP). Brush growth was carried out under ambient conditions using sacrificial metal surfaces with a larger oxidation potential than Cu^I/Cu^{II}, such as Zn, Al, Fe, and Co, which are all able to reduce Cu^{II} to Cu^I and to initiate polymerization. We also show that this novel method is convenient to prepare well-defined gradient polymer brushes with complex shapes.



Scheme 1. a) Experimental setup of the sandwiched architecture where polymerization can proceed with microliter volumes of droplet solution and digital photos of the Zn/Si substrate sandwich architecture (left) and the substrate in solution (right). b) The proposed mechanism of electrochemical-potential difference-induced surface-initiated ATRP: the reactive metal (Zn) reduces Cu^{II}/(bipy)₂ to Cu^I/(bipy)₂, which diffuses to the counter initiator-modified silicon substrate to catalyze ATRP.

Scheme 1a is of sa-ATRP and the experimental setup used herein. A reactive metal surface (Zn) and an initiator-modified substrate (silicon) were sandwiched face to face and fixed by screws to adjust the gap distance. By placing a single drop of polymerization solution, with volumes as small as 10 μL for a 0.5 cm² sample at 200 μm gap distance, containing Cu^{II}/(bipy)₂ and monomer (3-sulfopropyl methacrylate potassium salt, SPMA) at the edge of the parallel plates, the solution was automatically sucked into the gap owing to capillary forces. Zn has an oxidation potential of 0.76 V, while Cu^{II} → Cu^I has a reduction potential of 0.16 V (the presence of bipy ligand allowed for reduction of Cu^{II} to Cu^I, otherwise, Cu⁰ would be obtained) and thus, a redox reaction spontaneously occurred at the Zn surface leading to the reduction Cu^{II}/(Bipy)₂ to Cu^I/(Bipy)₂, shown by a brown-red color between the two substrates. Once generated, the Cu^I species

[*] J. Yan, B. Li, B. Yu, Prof. W. Liu, Prof. F. Zhou
State Key Laboratory of Solid Lubrication, Lanzhou Institute of
Chemical Physics, Chinese Academy of Sciences
Lanzhou 730000 (China)
E-mail: wmlu@licp.cas.cn
zhouf@licp.cas.cn

Prof. W. T. S. Huck
Radboud University Nijmegen,
Institute for Molecules and Materials
Heyendaalseweg 135, 6525 AJ Nijmegen (The Netherlands)
E-mail: w.huck@science.ru.nl

[**] Thanks for the financial support of the NSFC (21125316, 51175202),
973 project (2013CB632300), and the Chinese Academy of Sciences
(KJZD-EW-M01).

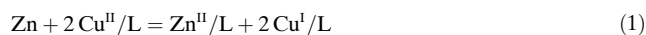
Supporting information for this article is available on the WWW
under <http://dx.doi.org/10.1002/ange.201304449>.

diffuse towards the initiator-modified substrate and initiate polymer-brush growth (Scheme 1 b).

The high concentration of Cu^{I} catalyst used in conventional aqueous ATRP always results in a large polymerization rate and high radical concentration, which increases the probability of chain termination. Moreover, the large halophilicity (K_{X}) of $\text{Cu}^{\text{II}}/\text{L}^{2+}$ and high concentration of X^- (where $\text{X} = \text{halogen}$) counteracts the dissociation of the deactivator and so lowers the deactivation efficiency in conventional ATRP. As shown in Scheme 1 b, sa-ATRP is initiated by an in situ formed concentration gradient of $\text{Cu}^{\text{I}}/(\text{bipy})_2$ (with the highest concentration near the anode) and hence, brush growth rates are determined by the distance between the two surfaces. Figure 1 a shows this dependence of polymer-brush growth on gap distance (D): when D was 0.34 mm, the polymerization showed fast growth (approximately 130 nm h^{-1}) and leveled off after 3.5 hours. When D was 0.78 mm, the polymerization was much more controlled (approximately 40 nm h^{-1}) and linear growth lasted for up to 6.5 hours. Increased control was attributed to the higher $\text{Cu}^{\text{II}}/\text{Cu}^{\text{I}}$ ratio at a larger gap distance. Figure 1 b shows how the thickness of PSPMA brushes was controlled by varying D (0.78 mm or 0.34 mm) and allowing the polymerization to proceed for 0.5 h or 1 h, respectively.

Bringing Zn in contact with a $\text{Cu}^{\text{II}}/(\text{bipy})_2$ solution sets up a potential difference and leads to a redox reaction, according to Equation (1), with the actual electric potential expressed as Equation (2). The polymerization rate in ATRP can be expressed as Equation (3); combining Equations (2) and (3) allows us to directly relate the rate of polymerization (rate of brush growth) to the redox potential. These equations also show how an increase in $\text{Cu}^{\text{II}}/(\text{bipy})_2$ concentration will

increase the $\text{Zn}/\text{Cu}^{\text{II}}(\text{bipy})_2$ potential difference and thus, accelerate the generation of $\text{Cu}^{\text{I}}/(\text{bipy})_2$, and hence the polymerization rate.



$$E = E_0 - \frac{RT}{nF} \ln \frac{[\text{Zn}^{\text{II}}/\text{L}][\text{Cu}^{\text{I}}/\text{L}]^2}{[\text{Cu}^{\text{II}}/\text{L}]^2} \quad (2)$$

$$R_p = k_p K_{\text{ATRP}} \left(\frac{[\text{P}_n\text{X}][\text{Cu}^{\text{I}}/\text{L}][\text{M}]}{[\text{X}/\text{Cu}^{\text{II}}/\text{L}]} \right) \quad (3)$$

Figure 1 c shows the variation of polymer thickness at different $\text{Cu}^{\text{II}}/(\text{bipy})_2$ concentrations and a fixed polymerization time of 0.5 h and fixed D of 0.34 mm. At very low $\text{Cu}^{\text{II}}/(\text{bipy})_2$ concentration, polymer growth was very slow owing to the very small amount of Cu^{I} activators generated. By increasing the concentration of $\text{Cu}^{\text{II}}/(\text{bipy})_2$, the brush thickness also increased dramatically until the concentration reached 0.5 mg mL^{-1} . Beyond that concentration, the thickness of the polymer brushes declined.

Notably, because of the small amount of grafted polymer and the overall small volumes used, it is not possible to determine the molecular weight (M_n) and polydispersity index (PDI) of the polymer brushes directly.^[14] Instead, we carried out polymer-brush swelling experiments to compare the grafting density differences of PSPMA brushes prepared by conventional Cu^{I} mediated ATRP and electrochemical-potential difference-induced ATRP. It was found that polymer brushes grown by sa-ATRP had a larger swelling ratio ($h_{\text{swollen}}/h_{\text{dry}} = 3.3$) than polymer brushes fabricated by conventional SI-ATRP ($h_{\text{swollen}}/h_{\text{dry}} = 2.4$; Supporting Information,

Figure S4). The swelling ratio of the polyelectrolyte brushes was linearly related to the degree of polymerization,^[15] which led us to conclude that sa-ATRP yielded polymer brushes with a lower grafting density.

Gradient surfaces have potential applications for studies of biological interactions, microfluidic devices, and sensors where topography plays an important role.^[16,17] They have been fabricated by a range of lithographic methods combined with self-assembled monolayers and surface-initiated polymerization (SIP).^[18,19] Herein, we created a gradient in Cu^{II} ion concentration by placing the Zn substrate at a tilt angle (θ) with respect to the initiator-modified substrate (Figure 2 a). Each point on this substrate along the y -direction will have a different $\text{Cu}^{\text{II}}/\text{Cu}^{\text{I}}$ ratio and therefore different polymer-growth kinetics. Figure 2 a (right) shows digital photographs and height profiles of gradient brushes obtained at two different tilt angles. The color changes are interference colors of different polymer thicknesses where the maximum polymer thicknesses are 65 nm (for $\theta = 11.5^\circ$) and 100 nm (for $\theta = 18.5^\circ$) in about one millimeter range. Gradient formation can be combined with patterning of the sacrifi-

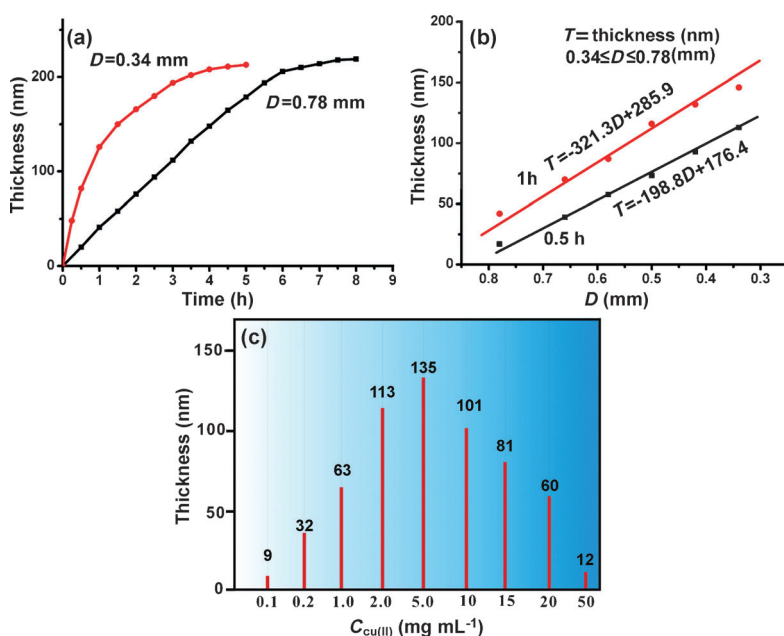


Figure 1. a) First-order kinetics with respect to PSPMA growth on initiator-modified Si surfaces with varying D . b) Polymer-thickness variation at different gap distances (D) in 0.5 h and 1 h. c) Thickness of PSPMA brushes at different $\text{Cu}^{\text{II}}/(\text{bipy})_2$ concentrations at 0.5 h sa-ATRP and $D = 0.34 \text{ mm}$.

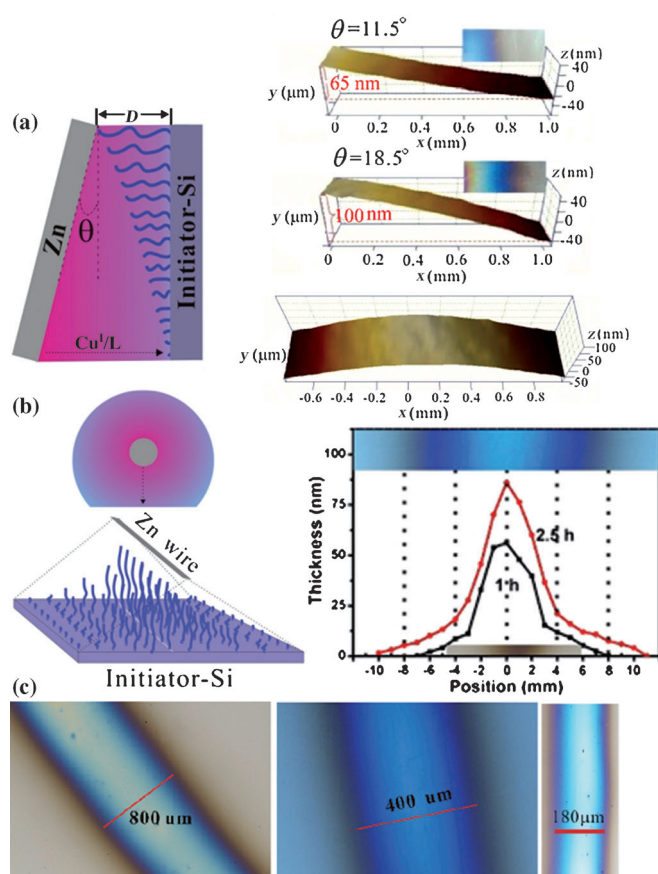


Figure 2. a) Scheme of gradient polymer brushes with a tilted Zn slice ($\theta = 11.5^\circ$ or 18.5°). b) A single Zn wire anode results in a ridge-like polymer brush structure and profiles. Upper right: digital photograph of the gradient polymer architecture. Bottom right: graph of the distribution of polymer thickness ($D = 0.78$ mm). c) The lateral size of the polymer-brush gradient can be changed by gradually reducing the size of the Zn wires.

cial Zn surface. When a Zn wire is placed above substrates at a distance of 0.78 mm, a ridge-like $\text{Cu}^{\text{I}}/\text{Cu}^{\text{II}}$ gradient will be formed, as illustrated in Figure 2b. The minimum pattern size obtainable depends on the size of the Zn slice and on the polymerization time. At longer polymerization times, the continuously generated catalyst diffuses farther in the lateral directions (20 mm brush pattern width in 2.5 hours, but only with 14 mm in 1 h). Figure 2c shows how line widths as small as 180 μm can be obtained.

By changing the shape of the Zn slice, polymer brushes can be “painted” in different shapes. Zn substrates patterned into different shapes translated into patterned brushes of the same shape (cross, triangle, letters, and Y shape) as a result of the catalyst distribution governed by the Zn, also shown in digital photographs (Figure 3a). Complex shapes of polymer brushes could also be made by masking the Zn slice with elastomer films (Figure 3b). A thin PDMS film of 200 μm in a Y shape was applied to the Zn substrate and then the Y-shape channel was filled with the polymerization solution (5 μL). After the initiator-modified substrate was in tight contact with the PDMS film, in situ polymerization occurred in the confined space to yield polymer brushes with a Y shape

(Figure 3b, bottom left). The brush surface provides a unique substrate with different wettabilities forming a simple in-plane gravity-driven microfluidic device^[20] where two water droplets from the branches of the Y moved along the Y-shaped channel under gravity before merging. Following this strategy, sa-ATRP has the advantage of carrying out polymerizations of multiple monomers on a single surface. A number of channels were cast in the PDMS film, which was placed on top of the Zn substrate (Figure 3c). In each channel, a monomer solution was added and an instantaneous redox reaction occurred to catalyze the polymerization. Once an initiator-modified substrate was placed on top of the monomer-filled channels, multiple polymer brushes grew from this substrate. Up to six polymer brushes were formed on a silicon surface with a total volume of 50 μL monomer solution (Figure 3c; the different thicknesses result from different grafting kinetics).

In summary, we have exploited the electrochemical potential difference between reductive metals and a $\text{Cu}^{\text{II}}/\text{L}$ solution to generate a $\text{Cu}^{\text{I}}/\text{L}$ catalyst that initiates surface-bound ATRP. This method allows polymer-brush growth in a metal-substrate sandwiched architecture in air, using volumes as small as 5 μL , in which Cu^{I} activators are continuously generated and diffusively transported to the initiator-modified substrate. Polymer-brush gradients and complex shapes were easily generated by spatially distributing the generation of the catalyst. The advantage of this approach is that polymerizations of minute quantities of multiple monomers on a single surface can easily be achieved and many polymer brushes can be formed simultaneously using sa-ATRP. This method shows potential for applications involving expensive or hard-to-synthesize monomers and in screening the properties of many (co-)polymer brushes simultaneously.

Experimental Section

The silicon wafer was washed with distilled water, ethanol, and acetone under ultrasound conditions, and then was activated using oxygen plasma for minutes to realize surface hydroxylation. The as-prepared substrates were placed in a vacuum desiccator with a vial containing 5 μL of 3-(trichlorosilyl)propyl-2-bromo-2-methylpropanoate, the chamber was then pumped down to less than 1 mbar and kept under vacuum for 20 min with 3 cycles.

Preparation of polymer brushes: Monomer solution was made of 3-sulfopropyl methacrylate potassium salt (SPMA, 95 %, TCI), $\text{CuCl}_2 \cdot 2\text{H}_2\text{O}$ (AR, Tianjin, China). Bipyridyl (35 mg), $\text{CuCl}_2 \cdot 2\text{H}_2\text{O}$ (13 mg), and 3-sulfopropyl methacrylate potassium salt (SPMA) monomer (3 g) were charged in a quartz flask, then a solution of $\text{H}_2\text{O}/\text{MeOH}$ (5 mL, 2:1 (v/v)) was added. The initiator-modified silicon wafer was cut to about 15 mm \times 8 mm, and a commercially available Zn sheet was sanded with abrasive paper to remove the oxide layer and then was cut to 15 mm \times 8 mm. Four screws were used to fix the two substrates into a sandwiched architecture and to adjust the distance (D) between them.

Fabrication of gradient polymer brushes and writing directly on the silicon wafer: The Zn slice was cut into about 1.0 mm width to fabricate the gradient polymer brushes ($D = 780$ μm), when used in writing letters, $D = 200$ μm .

The degassed precursor of silicone (Sylgard 184) was poured onto the Zn slice and cured at 80 $^\circ\text{C}$ for about 2 h. The PDMS layer can be carved to different patterns, then a small volume of solution was

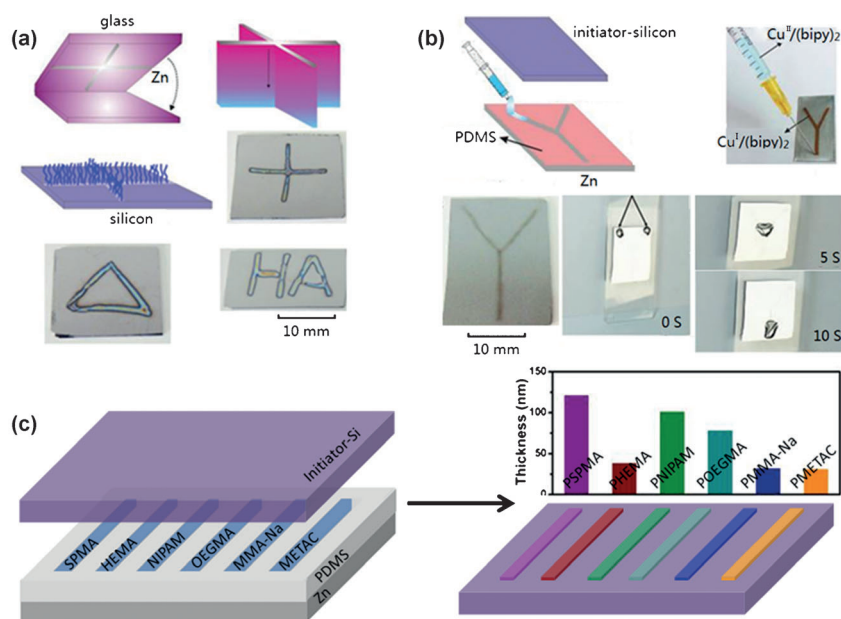


Figure 3. a) Preparation of patterned polymer growth by varying the shape of the Zn slice and the spatial distribution of the catalyst. Schematic set-up, model of the distribution of catalysis, and digital photographs of PSPMA brushes on a Si substrate (2 h polymerization). b) An in-plane microfluidic device made of Y-shaped PSPMA brushes (0.5 h polymerization): PDMS sheet was carved Y shape and masked onto Zn slice. Top right: Digital photograph of the redox reaction that occurs when a drop of solution was added. Bottom: Digital photographs of masked polymer grafting on initiator-silicon was clapped onto PDMS (left) and the microfluidic experiment (right, 3 photographs). c) Fabrication of many different polymer brushes on a single substrate and the thickness of the as-prepared polymer brushes after 1 h polymerization. Each channel was filled with one monomer solution: SPMA=3-sulfopropyl methacrylate potassium salt; HEMA=2-hydroxyethyl methacrylate; MAA-Na=sodium methacrylate; NIPAM=N-isopropyl acrylamide; OEGMA=oligo(ethyleneglycol) methacrylate; METAC=methacryloylcholine chloride.

dipped into the groove to contact the Zn for polymer growth on the Si substrate.

The thicknesses of the polymer films were measured using an L116E ellipsometer (Gaertner, USA) equipped with a He–Ne laser source (632.8 nm at an incident angle of 50°) with a refractive index of 1.46. Optical images of the gradient polymer brushes were taken with a NanoMap 500 LS 3D profilometer (AEP Technology, USA). Atomic force microscopy (AFM) measurements were performed on an Agilent Technologies 5500AFM in tapping mode using a pyramidal Si tip (Veeco, RTEP). Chemical composition information was obtained by X-ray photoelectron spectroscopy (XPS) measurement on a PHI-5702 multifunctional spectrometer using Al K α radiation, and the binding energies were referenced to the C1s at 284.8 eV from adventitious carbon.

Received: May 23, 2013

Published online: July 1, 2013

Keywords: gradient · polymer brushes · polymerization · sacrificial anodes · surface-initiated polymerization

- [1] a) J.-S. Wang, K. Matyjaszewski, *J. Am. Chem. Soc.* **1995**, *117*, 5614; b) K. Matyjaszewski, J. Xia, *Chem. Rev.* **2001**, *101*, 2921; c) X. Chen, S. P. Armes, *Adv. Mater.* **2003**, *15*, 1558; d) M. A. C. Stuart, W. T. S. Huck, J. Genzer, M. Müller, C. Ober, M. Stamm, G. B. Sukhorukov, I. Szleifer, V. V. Tsukruk, M. Urban, F.

- Winnik, S. Zauscher, L. Luzinov, S. Minko, *Nat. Mater.* **2010**, *9*, 101.
[2] a) C. Tonhauser, A. A. Golriz, C. Moers, R. Klein, H. Butt, H. Frey, *Adv. Mater.* **2012**, *24*, 5559; b) X. Liu, Q. Ye, B. Yu, Y. Liang, W. Liu, F. Zhou, *Langmuir* **2010**, *26*, 12377; c) H. Ma, J. Hyun, P. Stiller, A. Chilkoti, *Adv. Mater.* **2004**, *16*, 338; d) O. Azzaroni, A. A. Brown, W. T. S. Huck, *Adv. Mater.* **2007**, *19*, 151; e) C. Huang, N. D. Brault, Y. Li, Q. Yu, S. Jiang, *Adv. Mater.* **2012**, *24*, 1834; f) X. Laloyaux, E. Fautré, T. Blin, V. Purohit, J. Leprince, T. Jouenne, A. M. Jonas, K. Glinel, *Adv. Mater.* **2010**, *22*, 5024.
[3] a) Z. Zhang, S. Chen, S. Jiang, *Biomacromolecules* **2006**, *7*, 3311; b) A. Hucknall, S. Rangarajan, A. Chilkoti, *Adv. Mater.* **2009**, *21*, 2441.
[4] L. Sun, G. L. Baker, M. L. Bruening, *Macromolecules* **2005**, *38*, 2307.
[5] a) F. Zhou, W. Shu, M. E. Welland, W. T. S. Huck, *J. Am. Chem. Soc.* **2006**, *128*, 5236; b) F. Zhou, P. M. Biesheuvel, E.-Y. Choi, W. Shu, R. Poetes, U. Steiner, W. T. S. Huck, *Nano Lett.* **2008**, *8*, 725.
[6] a) R. Barbey, L. Lavanant, D. Paripovic, N. Schüwer, C. Sugnaux, S. Tugulu, H.-A. Klok, *Chem. Rev.* **2009**, *109*, 5437; b) T. Chen, R. Ferris, J. Zhang, R. Ducker, S. Zauscher, *Prog. Polym. Sci.* **2010**, *35*, 94; c) J. L. Dalsin, B.-H. Hu, B. P. Lee, P. B. Messersmith, *J. Am. Chem. Soc.* **2003**, *125*, 4253; d) I. E. Dunlop, W. H. Briscoe, S. Titmuss, R. M. J. Jacobs, V. L. Osborne, S. Edmondson, W. T. S. Huck, J. Klein, *J. Phys. Chem. B* **2009**, *113*, 3947; e) D. Bontempo, N. Tirelli, K. Feldman, G. Masci, V. Crescenzi, J. A. Hubbell, *Adv. Mater.* **2002**, *14*, 1239.
[7] S. Edmondson, V. L. Osborne, W. T. S. Huck, *Chem. Soc. Rev.* **2004**, *33*, 14.
[8] a) Z. H. Nie, E. Kumacheva, *Nat. Mater.* **2008**, *7*, 277; b) R. Ducker, A. Garcia, J. M. Zhang, T. Chen, S. Zauscher, *Soft Matter* **2008**, *4*, 1774; c) S. Schilp, N. Ballav, M. Zharnikov, *Angew. Chem.* **2008**, *120*, 6891; *Angew. Chem. Int. Ed.* **2008**, *47*, 6786; d) M. Steenackers, A. Kueller, N. Ballav, M. Zharnikov, M. Grunze, R. Jordan, *Small* **2007**, *3*, 1764; e) T. Winkler, N. Ballav, H. Thomas, M. Zharnikov, A. Terfort, *Angew. Chem.* **2008**, *120*, 7348; *Angew. Chem. Int. Ed.* **2008**, *47*, 7238; f) X. Q. Liu, Y. Li, Z. J. Zheng, *Nanoscale* **2010**, *2*, 2614; g) X. Zhou, X. Wang, Y. Shen, Z. Xie, Z. Zheng, *Angew. Chem.* **2011**, *123*, 6636; *Angew. Chem. Int. Ed.* **2011**, *50*, 6506.
[9] a) K. Matyjaszewski, *Macromolecules* **2012**, *45*, 4015; b) W. Tang, Y. Kwak, W. Braunecker, N. V. Tsarevsky, M. L. Coote, K. Matyjaszewski, *J. Am. Chem. Soc.* **2008**, *130*, 10702; c) W. Tang, N. V. Tsarevsky, K. Matyjaszewski, *J. Am. Chem. Soc.* **2006**, *128*, 1598; d) F. Zhou, Z. Zheng, B. Yu, W. Liu, W. T. S. Huck, *J. Am. Chem. Soc.* **2006**, *128*, 16253.
[10] a) A. J. Magenau, N. C. Strandwitz, A. Gennaro, K. Matyjaszewski, *Science* **2011**, *332*, 81; b) N. Bortolamei, A. A. Isse, A. J. Magenau, A. Gennaro, K. Matyjaszewski, *Angew. Chem.* **2011**, *123*, 11593; *Angew. Chem. Int. Ed.* **2011**, *50*, 11391.
[11] a) M. A. Tasdelen, M. Ciftci, Y. Yagci, *Macromol. Chem. Phys.* **2012**, *213*, 1391; b) B. P. Fors, C. J. Hawker, *Angew. Chem.* **2012**, *124*, 8980; *Angew. Chem. Int. Ed.* **2012**, *51*, 8850; c) C. J. Wallentin, J. D. Nguyen, P. Finkbeiner, C. R. Stephenson, J.

- Am. Chem. Soc.* **2012**, *134*, 8875; d) D. Konkolewicz, K. Schröder, J. Buback, S. Bernhard, K. Matyjaszewski, *ACS Macro Lett.* **2012**, *1*, 1219; e) M. A. Tasdelen, M. Uygün, Y. Yagci, *Macromol. Chem. Phys.* **2011**, *212*, 2036; f) Y. Yagci, S. Jockusch, N. J. Turro, *Macromolecules* **2010**, *43*, 6245; g) E. H. H. Wong, S. N. Guntari, A. Blencowe, M. P. van Koe-verden, F. Caruso, G. G. Qiao, *ACS Macro Lett.* **2012**, *1*, 1020; h) N. V. Alfredo, N. E. Jalapa, S. L. Morales, A. D. Ryabov, R. L. Lagadec, L. Alexandrova, *Macromolecules* **2012**, *45*, 8135; i) F. A. Leibfarth, K. M. Mattson, B. P. Fors, H. A. Collins, C. J. Hawker, *Angew. Chem.* **2013**, *125*, 210; *Angew. Chem. Int. Ed.* **2013**, *52*, 199.
- [12] a) A. Simakova, S. E. Averick, D. Konkolewicz, K. Matyjaszewski, *Macromolecules* **2012**, *45*, 6371; b) J. K. Oh, K. Min, K. Matyjaszewski, *Macromolecules* **2006**, *39*, 3161.
- [13] a) B. Li, B. Yu, W. T. S. Huck, F. Zhou, W. Liu, *Angew. Chem.* **2012**, *124*, 5182; *Angew. Chem. Int. Ed.* **2012**, *51*, 5092; b) B. Li, B. Yu, W. T. S. Huck, W. Liu, F. Zhou, *J. Am. Chem. Soc.* **2013**, *135*, 1708.
- [14] S. Turgman-Cohen, J. Genzer, *J. Am. Chem. Soc.* **2011**, *133*, 17567.
- [15] Y. Tran, P. Auroy, L.-T. Lee, *Macromolecules* **1999**, *32*, 8952.
- [16] a) Y. Mei, T. Wu, C. Xu, K. J. Langenbach, J. T. E. D. Vogt, K. L. Beers, E. J. Amis, N. R. Washburn, *Langmuir* **2005**, *21*, 12309; b) T. Chen, I. Amin, R. Jordan, *Chem. Soc. Rev.* **2012**, *41*, 3280; c) R. R. Bhat, B. N. Chaney, J. Rowley, A. Liebmann-Vinson, J. Genzer, *Adv. Mater.* **2005**, *17*, 2802.
- [17] a) J. Genzer, R. R. Bhat, *Langmuir* **2008**, *24*, 2294; b) C. Xu, S. E. Barnes, T. Wu, D. A. Fischer, D. M. DeLongchamp, J. D. Batteas, K. L. Beers, *Adv. Mater.* **2006**, *18*, 1427; c) M. N. Khan, V. Tjong, A. Chilkoti, M. Zharnikov, *Angew. Chem.* **2012**, *124*, 10449; *Angew. Chem. Int. Ed.* **2012**, *51*, 10303.
- [18] a) S. Christian, S. Svetlana, P. Oswald, J. Rühle, *Adv. Mater.* **2009**, *21*, 4706; b) M. Steenackers, A. Küller, S. Stoycheva, M. Grunze, R. Jordan, *Langmuir* **2009**, *25*, 2225.
- [19] X. Lin, Q. He, J. Li, *Chem. Soc. Rev.* **2012**, *41*, 3584.
- [20] I. You, S. M. Kang, S. Lee, Y. O. Cho, J. B. Kim, S. B. Lee, Y. S. Nam, H. Lee, *Angew. Chem.* **2012**, *124*, 6230; *Angew. Chem. Int. Ed.* **2012**, *51*, 6126.